Variable patterns of local adaptation along an elevation gradient in a host-pathogen interaction

Michael Rechsteiner[1,2], Fletcher W. Halliday[2,3], Michael Giolai[1], Andreas Wagner[2,4,5], Anna-Liisa Laine[1]

[1]Research Centre for Ecological Change, Organismal and Evolutionary Biology Research Programme, Faculty of Biological and Environmental Sciences, University of Helsinki, Helsinki, Finland

[2]Department of Evolutionary Biology and Environmental Studies, University of Zürich, Zürich, Switzerland

[3]Department of Botany and Plant Pathology, Oregon State University, Corvallis, Oregon, USA

[4]Swiss Institute of Bioinformatics, Quartier Sorge-Batiment Genopode, Lausanne, Switzerland

[5]The Santa Fe Institute, Santa Fe, New Mexico, USA

Corresponding author: Michael Rechsteiner (michael.rechsteiner@helsinki.fi)

Keywords: Elevation gradient, coevolution, plant-pathogen interactions, local adaptation, species interactions, host-parasite interactions

Abstract

The strength of biotic interactions is hypothesized to decrease with elevation, yet it remains unclear whether this decline results in weaker selection at higher elevations. Further, it is not known if varying ecological interactions along elevation gradients affect the patterns of local adaptation between hosts and pathogens. Here, we experimentally test whether the direction

and strength of local adaptation vary between four populations of a host and its specialist fungal pathogen along an elevation gradient. This system represents a steep climatic gradient and is characterized by variation in infection prevalence along altitude, where infected plants are rarely observed in the highest elevation population. We measured infection success and severity across several hundred plant-pathogen pairs and tested for differences between sympatric and allopatric host-pathogen combinations. We found signs of both local adaptation and maladaptation in the severity of infections between populations. The high-elevation pathogen population was locally adapted, whereas the low-elevation pathogen population was locally maladapted. Our results suggest a relationship between varying pathogen prevalence and the pattern of local adaptation along an environmental gradient, highlighting that climate driven shifts in pathogen distributions may reshape coevolutionary dynamics between hosts and pathogens.

Introduction

The hypothesis that the intensity of biotic interactions varies predictably with latitude and elevation was first proposed by Darwin (Darwin, 1859), and has since gained considerable empirical support (Hargreaves et al., 2020; Zvereva & Kozlov, 2021, 2022). The intensity of species interactions, such as encounter rates or the transmission probability of pathogens, is expected to scale with community productivity and species abundance, both of which decline toward higher elevations (Hargreaves et al., 2019; Roslin et al., 2017). Indeed, ecological networks are more connected at lower elevations (Ho et al., 2022). Further, both theoretical predictions and empirical results show that interaction intensity is consistently related to the strength of selection acting on traits mediating species interactions (Arnold & Wade, 1984; Benkman, 2013). Thus, coevolutionary selection should be stronger at lower elevations and latitudes (Hochberg & Baalen, 1998). Building on this idea, the geographic mosaic theory of

coevolution emphasizes that spatial variation in abiotic and biotic conditions can alter the strength and direction of reciprocal selection among interacting species, potentially leading to locally divergent or even opposing evolutionary outcomes across landscapes (Gomulkiewicz et al., 2000; Thompson, 2005). Yet, studies that leverage environmental gradients to study coevolutionary processes remain rare (but see Toju, 2008; King *et al.*, 2009; Lopez-Pascua *et al.*, 2010).

Environmental conditions, such as temperature, can profoundly alter the evolutionary dynamics of hosts and pathogens (Wolinska & King, 2009), for instance, by shifting how traits important for interactions are expressed across environments, through genotype-by-environment interactions, or by differential effects of the environment on host and pathogen performance. Hence, we expect the relationship between hosts and pathogens to vary along environmental gradients. Across elevation gradients, associated changes in host density can impact pathogen distributions (McNew et al., 2021; Pulgarín-R et al., 2018) which might generate potential for eco-evolutionary feedbacks (Ashby et al., 2019). Further, the steep decline in temperature is considered to be another key driver generating variation in biotic interactions (Körner, 2003; Louthan et al., 2015). The role of the environment as a major determining factor of diseases was first proposed in the 1960s by the concept of the disease triangle, which highlights the interplay between host, pathogen, and the environment in determining infection outcomes (George McNew, 1960; Stevens, 1960). Infection severity, disease prevalence, and the duration of an epidemic may all be affected by environmental conditions, and disease prevalence has indeed been shown to both increase or decrease along elevation gradients (Abbate & Antonovics, 2014; Halliday et al., 2021). To identify the role of the environment in mediating host-pathogen coevolution, environmental variation has been incorporated into experimental evolution studies that have demonstrated that coevolutionary

selection can both be intensified and constrained by environmental variation (Lopez-Pascua & Buckling, 2008; Harrison *et al.*, 2013; Duncan *et al.*, 2017). In sum, elevation gradients represent valuable systems to study ecological and evolutionary processes between hosts and pathogens.

Local adaptation assays are powerful tools for detecting signatures of coevolution between hosts and pathogens (Blanquart et al., 2013; Kawecki & Ebert, 2004). In such assays, pathogen virulence and host resistance are measured and compared between sympatric and allopatric host and pathogen populations. In plant-pathogen interactions, host resistance and pathogen virulence often manifest in two forms: qualitative, where specific host–pathogen genotype combinations result in either successful infection or no infection at all (i.e., a binary compatible/incompatible outcome) (Jones & Dangl, 2006), and quantitative, where infection occurs but pathogen growth, reproduction, or transmission is reduced (McDonald & Linde, 2002; Poland et al., 2009). Differences in virulence and resistance indicate that hosts or pathogens are either adapted or maladapted to their native interaction partners. Local adaptation is strongly dependent on migration rate (Greischar & Koskella, 2007; Hoeksema & Forde, 2008), spatial structure (Thrall & Burdon, 1997), and environmental heterogeneity (Wolinska & King, 2009). Therefore, we can expect coevolutionary trajectories to vary along elevation gradients. Such geographic variation in selection strength and interaction intensity is captured by the concept of coevolutionary hot and cold spots (Gomulkiewicz et al., 2000; Thompson, 2005), resulting in a mosaic of local adaptations among populations.

Here, we investigate whether patterns of infection pressure and local adaptation vary among populations of the host plant *Plantago lanceolata* and its powdery mildew pathogens distributed along an elevation gradient in the southeastern Swiss Alps. Elevation gradients are

associated with substantial abiotic and biotic variation and therefore provide a useful framework for examining how ecological context may shape the outcome of host pathogen interactions across landscapes. Among the focal populations, some showed consistently higher infection pressure, estimated from host density and pathogen prevalence, while others showed lower infection pressure. To examine whether patterns of local adaptation also varied among populations, we performed reciprocal infection experiments using host plants and pathogen isolates originating from the same populations and measured infection success and infection severity as proxies for pathogen fitness. We observed no significant differences in qualitative infection outcomes among pathogen and host populations. In contrast, quantitative infection outcomes varied among population pairs: infections were most severe in the high elevation population combinations and least severe in the low infection pressure populations. These patterns parallel the observed differences in infection pressure among populations and are consistent with geographic mosaic theory, which predicts spatial variation in the strength and outcome of host pathogen interactions (Thompson, 2005).

Methods

Study system and field data collection

Our focal host species, *Plantago lanceolata,* is an obligately outcrossing, perennial herbaceous plant in the order of *Lamiales. Plantago lanceolata* is native to Europe and Western Asia, but has been introduced and established in countries on every continent except Antarctica (Alexander et al., 2012; Penczykowski & Sieg, 2021). In the Swiss Alps, *P. lanceolata* typically occurs in montane and subalpine grasslands (Lauber et al., 2018).

Plantago lanceolata is a host of *Podosphaera plantaginis* (Castagne; U. Braun and S. Takamatsu), a powdery mildew fungus in the order *Erysiphales* within the Ascomycota. It is a

specialized pathogen that only infects a few species of the *Plantaginacea* family and requires living host tissue through its whole life cycle (Bushnell, 2002). An infection begins when ascospores germinate on the host surface, followed by mycelial growth visible to the naked eye and the development of haustorial roots that parasitize host cells (Bushnell, 2002). *Podosphaera plantaginis* reproduces both asexually and sexually. Asexual reproduction occurs via the development of haploid conidial spores, dispersed by wind, which may germinate after contact with a compatible host. Sexual reproduction occurs through the formation of chasmothecia, initiated by hyphal fusion either within a single individual (selfing) or between coinfecting individuals (outcrossing). Inside the chasmothecium, haploid ascospores develop following meiosis of the diploid zygote. Chasmothecia are typically formed at the end of a growing season and represent the overwintering life stage in seasonal environments. At the onset of the following season, chasmothecia rupture and initiate a new outbreak through the release of ascospores (Tack & Laine, 2014; Tollenaere & Laine, 2013).

We focus our study on four host and pathogen populations along the southern slope of Mount Calanda (46°53′59.5″N 9°28′02.5″E) in the Swiss Alps. These populations inhabit calcareous grasslands at approximately 700 m (low elevation), 1000 m (mid-low), 1400 m (mid-high), and 1700 m (high), and are separated by forests and rocky terrain (Fig. 1A). Along this slope, temperature decreases by 0.57°C per 100 m increase in elevation (Halliday et al., 2021), creating thermal variation among the grassland populations which may constrain the performance of both host and pathogens, and may additionally affect coevolutionary processes between our study species (Wolinska & King, 2009). To gain information on the distribution of both focal species along the elevation gradient, we collected density data of *P. lanceolata* plants and powdery mildew-infected plants from 2019-2021. Our study grassland populations are grazed by cattle twice per season, which is a typical form of extensive land use in the Swiss

Alps (Bätzing, 2015). Every population was surveyed in late June to estimate *P. lanceolata* density after the first grazing when the vegetation was low to accurately count plant individuals. In September, before the second grazing, we estimated the disease prevalence. Both surveys were conducted within 22 sites across all populations, each with an area of 2500 m^2 (Figure 1A, Halliday *et al.*, 2021). To measure plant density, the number of *P. lanceolata* individuals was counted at nine $4m^2$ plots that are arranged within each site in an equally spaced 3x3 grid. A more detailed outline of the plot layout within a site is described in Halliday *et al.* (2021). The mildew prevalence survey was conducted during the first two weeks of September. In 2021, the high-elevation population was revisited in late September, because no infections had been observed during the early September survey. During a survey, a surveyor slowly walks through each site for one hour, observes host plants for visual mildew symptoms, and records the number of infected plants. Infections are identified by white mycelial lesions on the green parts of plants. Besides *P. plantaginis*, a second powdery mildew species, *Golovinomyces sordidus* (L. Junell) V. P. Heluta, can infect *P. lanceolata*. Both *P. plantaginis* and *G. sordidus* develop local epidemics in *P. lanceolata* populations on Mount Calanda (Rechsteiner, Giolai *et al*., unpublished data) and cause identical symptoms. Hence, the powdery mildew prevalence data does not discriminate between the two powdery mildew species, and the relative contribution of each species to the observed symptoms is not known.

Cross-infection experiment to test local adaptation

To test whether the patterns of local adaptation differ between our study populations along the elevation gradient, we collected plant seeds and infected leaves from each population along the elevation gradient for a reciprocal inoculation assay. Seeds from 15 mother plants per population were collected in August and September 2021. Mother plants were selected from 19 field survey sites, with each population represented by individuals originating from four or

five sites. This sampling strategy ensured broad spatial coverage within each population and provided a robust representation of genetic variation at each elevation. The collected seeds were planted in a 15 cm x 15 cm pot with a 1:1 soil:sand mixture and placed in a climate chamber at 21° C, 80% air humidity, and with a 16L/8D day cycle. If multiple seeds from the same mother plant germinated after two weeks, all but one randomly chosen seedling were weeded. The remaining seedlings, representing 60 different genotypes, were grown for six months into adult plants before harvesting leaves for the infection assay. To obtain wild isolates of *P. plantaginis*, leaves of infected plants from all four populations were collected within multiple field survey sites at Calanda in August and September 2021. To obtain genetically homogeneous powdery mildew isolates, multiple rounds of transferring conidial spores from small lesions onto fresh detached leaves of susceptible stock plants were performed (Laine, 2005). At the time of the experiment, 11 *P. plantaginis* isolates were viable (low elevation: N=2, mid-low elevation: N=4, mid-high elevation: N=2, high-elevation: N=3) representing one to three survey sites per population. We verified the species of collected isolates through the amplification of a universal fungal DNA barcode and subsequent Sanger sequencing (described in supp. methods). To then test whether our study populations differ in their degree of local adaptation, we measured the infection outcome of every possible pairwise combination of 60 plant genotypes and 11 *P. plantaginis* isolates (Fig. 1D).

To perform the experiment, detached leaves from all 60 plant genotypes were sterilized by washing for two minutes in 4% bleach and 30 seconds in 70% ethanol inside of a biosafety cabinet. Following sterilization, leaves were cut into equally sized pieces and placed on top of moistened filter papers inside petri-dishes. One petri-dish always contained three leaf pieces from three randomly chosen plant genotypes. For the inoculation, a fine paint brush was used to transfer conidial spores from one single isolate growing on stock plant leaves onto one leaf

196 piece (Nicot et al., 2002). Leaf pieces in the same petri-dish were inoculated with the same
197 pathogen isolate. After the inoculation, the petri-dishes with the infected leaf pieces were
198 placed into a climate chamber (MLR-351-h, Panasonic) at 21 °C with a 16L/8D cycle. We
199 chose this temperature as it is close to the thermal optimum (21.6 °C) of multiple powdery
200 mildew species (Chaloner et al., 2020). Every combination of plant genotype and mildew
201 isolate was repeated in a second experimental block two weeks after the first experiment to
202 ensure the replicability of infection measurements. To measure infection outcome, each leaf
203 was observed for signs of infection on days 3, 5, 7, 9, and 12 post-inoculation. The leaf pieces
204 remained green and viable throughout the experimental period. At every time point, the
205 infection was visually inspected under a dissecting microscope, and the infection severity was
206 quantified using the following categories adapted from Bevan et al. (1993): 0 = no signs of
207 infection, 1 = mycelial growth; 2 = sparse sporulation, invisible to the naked eye; 3 = sparse
208 sporulation, visible with the naked eye; 4 = heavy sporulation, colony size smaller than 0.5
209 cm^2; 5 = heavy sporulation, colony size larger than 0.5 cm^2. When no signs of infection was
210 found on any leaf piece during both blocks, the plant genotype was considered resistant.
211 Otherwise, the plant was considered susceptible. Using the infection severity categories, the
212 day when sporulation was first observed (Bevan's scale > 1), which is equivalent to the latent
213 period, was identified for each plant genotype pathogen isolate pair. On day 15 post-inoculation
214 of the first experimental block, every infected leaf was checked for the presence of
215 chasmothecia, which were recorded numerically as either present (1) or absent (0). These
216 recordings were conducted only during the first experimental block, as chasmothecia formation
217 requires an extended incubation periods that was not feasible within the time frame of the
218 second block. In sum, three measurements were recorded in both experimental blocks: the
219 infection outcome over both blocks (0 = resistant, 1 = susceptible), infection severity in five

ascending categories, and the latent period of the pathogen (day of sporulation onset). Chasmothecia presence was recorded in the first block only.

Statistical analysis

To test whether *P. lanceolata* abundance varies across populations and seasons, we fitted a linear mixed model (LMM) using *lme4* (Bates et al., 2015) with population, season, as well as their interaction as fixed effects, and survey site as a random effect. Similarly, we tested whether the number of infected plants varies across populations and seasons. To do this, we fitted a generalised linear mixed model (GLMM) with a negative binomial distribution using *glmmTMB* (Brooks et al., 2017) with the population and season as fixed effects. We did not include an interaction term between population and season, because in 2020, no infected plants were observed in the high-elevation population which means that the interaction term is not fully estimable. In addition, to account for variation in the number of *P. lanceolata* plants among sites, we included the log-transformed number of *P. lanceolata* as an offset term in the model. For both above-described models, we tested whether model assumptions were met using DHARMa (Hartig, 2025).

To test whether the direction and the magnitude of local adaptation vary among the four focal populations, we used a hurdle-type modelling approach. First, we analysed infection outcome (0 = resistant, 1 = susceptible), determined from combined observations across both experimental blocks, using a binomial GLMM with host population, pathogen population, and their interaction as fixed effects, and the plant genotype nested within site and population and the pathogen isolate nested within population as random effects (*glmmTMB*; Brooks *et al.*, 2017). Then, we restricted subsequent analysis to successful infections. For the first experimental block, where chasmothecia observations were available, we analysed

chasmothecia presence (0 = absent, 1 = present) using a binomial GLMM with identical model structure. For both experimental blocks, we analysed infection severity (Bevan's scale > 1), and latent period of the pathogen (day of sporulation onset) using experimental block, host population, pathogen population, and all their interaction as fixed effects, and the plant genotype nested within site and population as a random effect, and the pathogen isolate nested within population as a random effect, fitting a cumulative link GLMM (*ordinal*; Christensen, 2023) and a LMM (*lme4*; Bates *et al.*, 2015b), respectively. This model structure accounts for a block effect while retaining observations from both blocks.

For every model described above, we performed type II ANOVA χ^2 tests to determine whether any effects significantly affected any infection measurements (significance threshold $p < 0.05$; *car* package for Wald χ^2 tests for LMMs and binomial GLMMs; *RVAideMemoire* package (Herve, 2023) for likelihood ratio χ^2 tests for the cumulative link GLMM).

When a significant main effect was detected in the χ^2 tests, we calculated estimated marginal means for each effect level (i. e., host or pathogen populations, or experimental block), and performed post-hoc pairwise comparisons between the levels of the main effect (i. e. comparisons among pathogen and hosts populations, or experimental blocks) using the *emmeans* package (Lenth, 2022), with p-values adjusted for multiple comparisons using the Tukey method.

For significant interactions between host population and pathogen population, we additionally computed pairwise contrasts 1) among host populations conditional on each pathogen population, and 2) among pathogen populations conditional on each host population. These two groups of contrasts correspond to the local *vs.* foreign and home *vs*. away criteria of local

adaptation proposed by Kawecki & Ebert (2004). We note that the interpretation of these criteria, and therefore the inference of local adaptation, depend on the focal organism: pathogen populations infecting the same host population tests for the local *vs.* foreign criteria from the pathogen's perspective and home *vs.* away criteria from the host's perspective, and *vice versa* for the reverse contrast. Tukey corrections were applied separately within each level of the conditional factor. For significant interactions of host/pathogen populations and the experimental block, we computed pairwise contrasts between the experimental blocks conditional on the host or pathogen population. No Tukey corrections were applied for this test, because one single contrast (block one *vs*. block two) was tested.

All statistical analyses were performed with R version 4.2.3 (R core team, 2023).

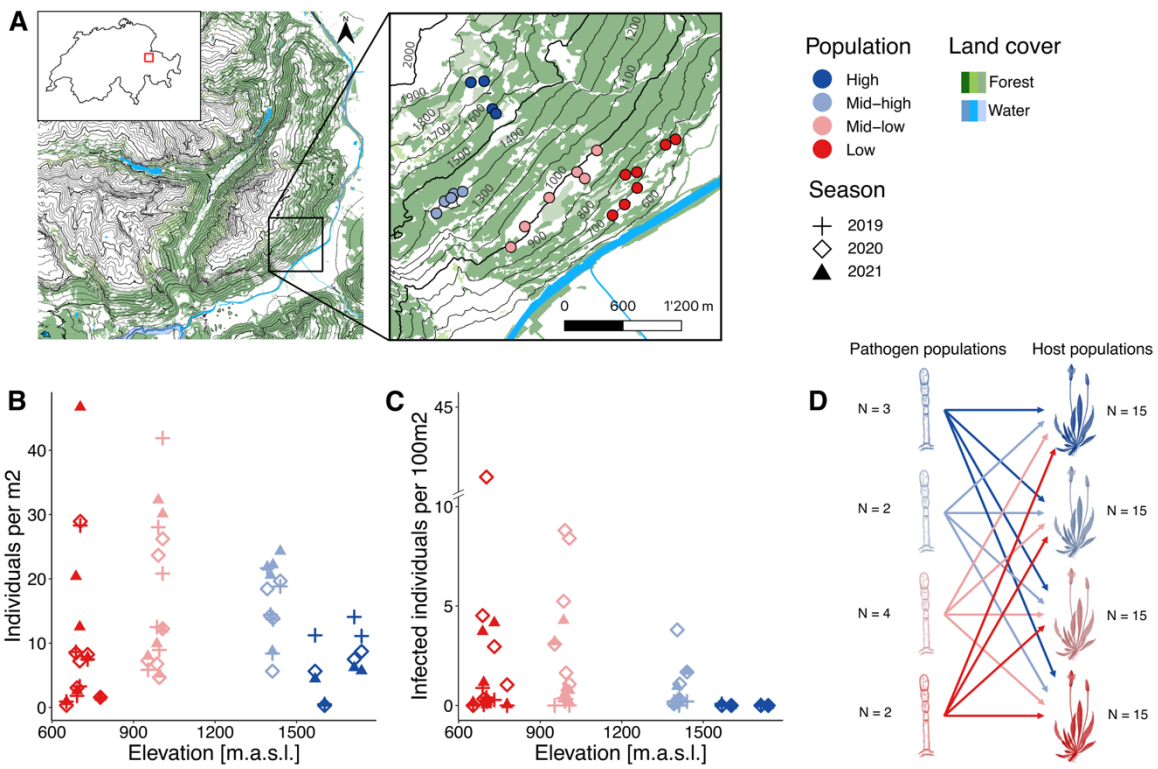

Figure 1: Map of study area, field survey data and experimental design. A) Topographic map depicting the location of the focal populations and survey sites in Eastern Switzerland. B) *P. lanceolata* density over three seasons. Each symbol represents the density of individuals observed at one site during one season. C) The density of powdery mildew infected *P. lanceolata* plants over three seasons. Each symbol represents the density of infected plants observed at one site during one season. D) Experimental design of the reciprocal infection study. Powdery mildew illustrations are adapted from Braun & Cook (2012), figure 109, page 155.

Results

Field survey

We surveyed montane and sub alpine grasslands to estimate the abundance of our focal host species and the prevalence of powdery mildew disease. In our field survey of host density during June 2019, 2020, and 2021, while lower density was observed at the low and high elevation populations, there were no significant differences between the study populations (χ^2 = 4.19, d. f. (degrees of freedom) = 3, p = 0.242, Supp. Table 1, Fig. 1B). However, seasonal variation was significant across all populations (χ^2 = 11.09, d. f. = 2, p = 0.004, Supp. Table 1, Supp. Table 2, Fig. 1B), yet the direction of change between seasons varied among populations (χ^2 = 22.69, d. f. = 6, p = 0.001, Supp. Table 1, Supp. Table 3, Fig. 1B). The low and mid-high elevation populations increased in density between 2020 and 2021 ($Season_{2020} - Season_{2021}$ = -4.95±1.79, d. f. = 36, p = 0.024, and $Season_{2020} - Season_{2021}$ = -5.16±2.12, d. f. = 36, p = 0.052, Supp. Table 3, Fig. 1B, respectively), the mid-high elevation increased between 2020 and 2021 ($Season_{2020} - Season_{2021}$ = -5.16±2.12, d. f. = 36, p = 0.052, Supp. Table 3, Fig. 1B), and while there is a decreasing trend in host density in the high elevation population, this trend is not supported statistically.

In our powdery mildew surveys during September 2019, 2020, and 2021, we found significant variation between study populations (χ^2 = 39.79, d. f. = 3, p < 0.001, Supp. Table 4, Fig. 1C)

and seasons (χ^2 = 32.81, d. f. = 2, p < 0.001, Supp. Table 4, Fig. 1C). In the low-elevation population, the number of infected plants was 4.13±1.82 times higher compared the mid-high elevation population (p = 0.003, Supp. Table 5, Fig. 1C), and 36.45±23.45 times higher compared to the high-elevation population (p < 0.001, Supp. Table 5, Fig. 1C). Similarly, the number of infected plants in the mid-low elevation population was 3.33±1.42 times higher compared to the mid-high elevation population (p = 0.025, Supp. Table 5, Fig. 1C), and 28.08±18.25 times higher compared to the high-elevation population (p < 0.001, Supp. Table 5, Fig. 1C). Finally, also the mid-high elevation population had 8.44±5.63 times the number of infected plants compared to the high-elevation population (p = 0.008, Supp. Table 5, Fig. 1D). Between seasons, in 2019, the number of infected plants was significantly lower compared to 2020 (ratio = 0.10±0.04, p <0.001, Supp. Table 5, Fig. 1C) and 2021 (ratio = 0.18±0.07, p <0.001, Supp. Table 5, Fig. 1C). In 2020, the number of infected individuals was highest, yet not significantly different from 2021 (ratio = 1.77±0.68, p = 0.302, Supp. Table 5, Fig. 1C).

Cross-infection experiment to test local adaptation

We inoculated 60 host genotypes from four grassland populations along an altitudinal gradient with 11 *P. plantaginis* isolates from the same populations in two separate experimental blocks to understand whether local adaptation varies in direction and magnitude across populations. In the resulting infection outcomes (0 = resistant, 1 <= susceptible) of 660 pairs host plant genotypes and pathogen isolates, we found that 172 pairs (~26%) are incompatible and 488 pairs (~74%) are compatible (Fig. 2). The patterns of compatibility (or incompatibility) between plant genotypes and pathogen isolates were highly genotype specific (Fig. 2). While most plant genotypes were susceptible to infection with *P. plantaginis*, some plant genotypes showed complete resistance against all tested isolates (e. g., I6-3), and others showed isolate specific resistance (e. g., U2-1 and U1-1). However, in our statistical analysis of the infection

outcome, we found no significant variation between the plant populations (χ^2 = 0.18, d. f. = 3, p = 0.981), the pathogen populations (χ^2 = 3.02, d. f. = 3, p = 0.389), or that the infection outcome depended both on the host and pathogen population respectively (χ^2 = 9.08, d. f. = 9, p = 0.430, Table 1, Fig. 3), which would indicate local adaptation. Most variation in the infection outcome model was explained by plant genotype and pathogen isolate, as indicated by the large difference between the conditional and marginal R^2 values (conditional R^2: 0.98, marginal R^2: 0.01, Supp. Table 6).

When focusing on successful infections over both experimental blocks (N=948), we found that infection severity varied significantly between plant populations and pathogen populations (LR χ^2 = 10.93, d. f. = 3, p = 0.012 and LR χ^2 = 9.57, d. f. = 3, p = 0.023, respectively). Both host and pathogen populations showed a consistent elevation gradient in infection severity, with high elevation populations showing the most severe infections, followed by mid-high, mid-low, and low elevation populations (host estimated mean category on a scale from 1 to 5: High = 4.29±0.09, Mid-high = 4.09±0.10, Mid-low = 3.90±0.13, and Low = 3.82±0.12; pathogen estimated mean category: High = 4.26±0.08, Mid-high = 4.07±0.10, Mid-low = 3.90±0.08, Low = 3.87±0.12). For both hosts and pathogens, pairwise comparisons between populations revealed that low- and mid-low elevation populations showed significantly lower odds of a more severe infection relative to their high elevation population (all OR < 0.36, all p < 0.05, Supp. Table 7, Fig. 4).

The effect of host and pathogen population on infection severity depended on each other (LR χ^2 = 18.91, d. f. = 9, p = 0.027, Table 2, Fig. 4), which indicates that the populations vary in their pattern of local adaptation. Within low elevation hosts, low -elevation pathogens produced the least severe infections, which were significantly less severe than infections with high-

elevation pathogens ($Low_{Pathogen}$ – $High_{Pathogen}$ OR = 0.28, OR 95% CI = [0.11, 0.72], p = 0.041, Supp. Table 8). In mid-low elevation hosts, low and mid-low elevation pathogens also caused less severe infections compared to high-elevation pathogens (Mid-$Low_{Pathogen}$ – $High_{Pathogen}$ OR = 0.32, OR 95% CI = [0.14, 0.71], p = 0.028, $Low_{Pathogen}$ – $High_{Pathogen}$ OR = 0.313, OR 95% CI = [0.121, 0.813], p = 0.08, Supp. Table 8). No significant differences among pathogen populations were found within mid-high elevation hosts. In high-elevation hosts, high-elevation pathogens caused the most severe infections, significantly more sever compared to mod-low elevation pathogens (Mid-$Low_{Pathogen}$ – $High_{Pathogen}$ OR = 0.14, OR 95% CI = [0.06, 0.31], p < 0.001, Supp. Table 8) and marginally the remaining pathogens (Mid-$high_{Pathogen}$ – $High_{Pathogen}$ OR = 0.31, OR 95% CI = [0.12, 0.80], p = 0.071, $Low_{Pathogen}$ – $High_{Pathogen}$ OR = 0.32, OR 95% CI = [0.12, 0.84], p = 0.095, Supp. Table 8).

From the pathogen perspective, low elevation pathogens caused more severe infections in high elevation hosts compared to low and mid-low elevation hosts (Low_{Host} - $High_{Host}$ OR = 0.144, OR 95% CI = [0.05, 0.46], p = 0.006, Mid-Low_{Host} - $High_{Host}$ OR = 0.196, OR 95% CI = [0.06, 0.63], p = 0.03, Supp. Table 8). While the mid-low pathogen population produced the least severe infection on their local host populations (Supp. Table 9), this was not supported statistically. The mid-high elevation pathogen population produced marginally more severe infections on high elevation hosts comparted to mid-low elevation hosts (Mid-Low_{Host} - $High_{Host}$ OR = 0.27, OR 95% CI = [0.09, 0.78], p = 0.075). Finally, the high elevation pathogen population produced the most severe infections on their local host population, significantly more severe than on low and mid-low (Low_{Host} - $High_{Host}$ OR = 0.163, OR 95% CI = [0.06, 0.45], p = 0.003, Mid-Low_{Host} - $High_{Host}$ OR = 0.20, OR 95% CI = [0.07, 0.57], p = 0.014), and marginally more severe on mid-high elevation hosts (Low_{Host} - $High_{Host}$ OR = 0.29, OR 95% CI = [0.11, 0.79], p = 0.073, Supp. Table 8).

We found no significant difference between the two experimental blocks (LR χ^2 = 0.172, D. f. = 1, p = 0.679, Table 1). There was, however, a significant interaction effect between the plant population and the experimental block (LR χ^2 = 9.009, D. f. = 3, p = 0.029, Table 1). The odds of a more severe infection were lower for mid-low elevation hosts in the first experimental block compared to the second experimental block (OR = 0.471, OR 95% CI = [0.268, 0.83], p = 0.009, Supp. Table 10).

Sporulation time was significantly affected by the plant populations (χ^2 = 7.97, D. f. = 3, p = 0.047), but not the pathogen population (χ^2 = 4.82, D. f. = 3, p = 0.185) or their interaction (χ^2 = 10.47, D. f. = 9, p = 0.314, Supp. Table 11). Pathogens sporulated earlier on high-elevation hosts compared to hosts from the lower-mid elevation (0.59±0.21 days earlier, p = 0.035, Supp. table 12, Supp. Fig. 1) and marginally earlier than hosts from the lowest elevation (0.49±0.21 days earlier, p = 0.093, Supp. table 12, Supp. Fig. 1).

Development of chasmothecia was not affected by the host population (χ^2 = 2.70, D. f. = 3, p = 0.440) or the pathogen population (χ^2 = 4.22, D. f. = 3, p = 0.239) but their interaction was marginally significant (χ^2 = 15.70, D. f. = 9, p = 0.074, Supp. Table 13). However, a post-hoc test did not reveal any significant differences among populations (data not shown). Nonetheless, the highest proportion of chasmothecia was observed in infections of high-elevation hosts (Supp. Fig. 2).

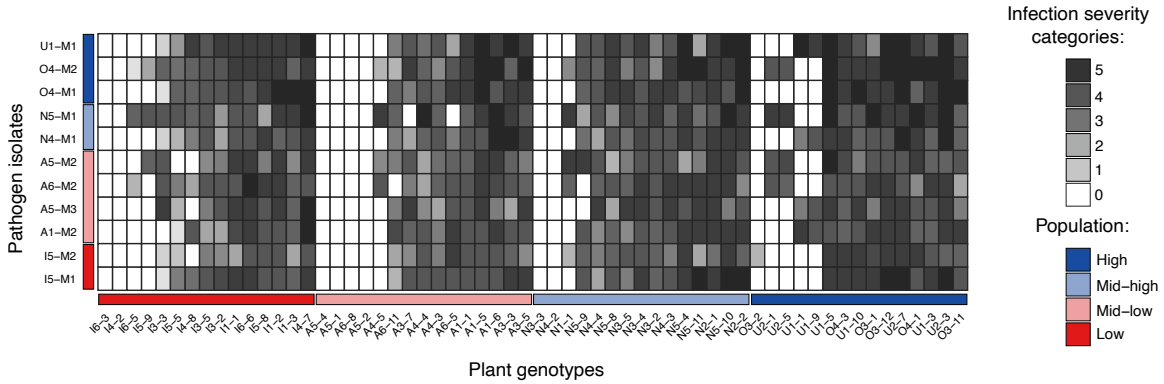

Figure 2: Infection severity at day 12 post-inoculation. Each square shows the infection severity calculated as the mean of one plant-pathogen pair between both experimental blocks. Each column shows the infection outcome of one single plant genotype infected with all mildew isolates and each row shows the infection outcome of a single mildew isolate on all plant genotypes. The colour bars indicate the origin population of plants and mildew isolates.

396

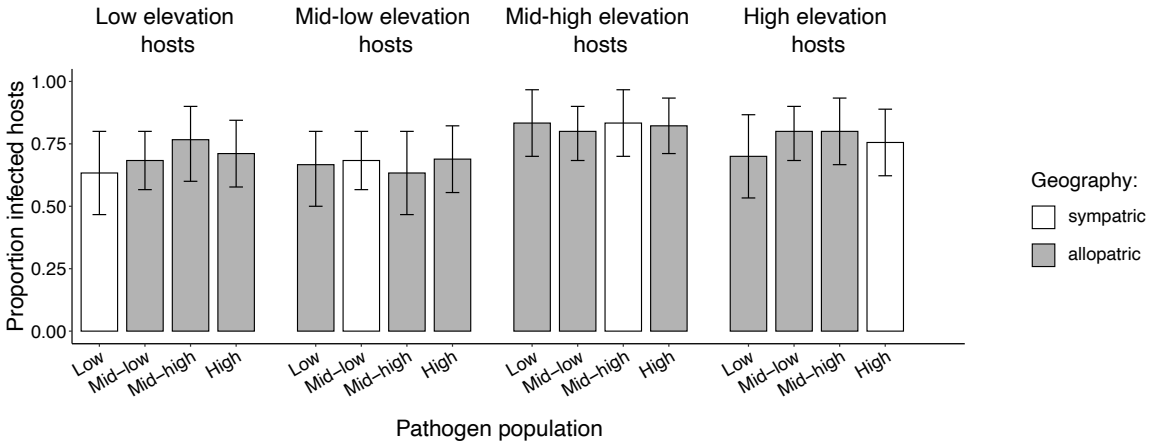

Figure 3: Proportion of successful infections of sympatric or allopatric host-pathogen pairings. Bar plot shows the proportion of infected hosts, with error bars indicating the standard error of the mean. Sympatric population combinations are marked in dark grey and allopatric in grey.

397

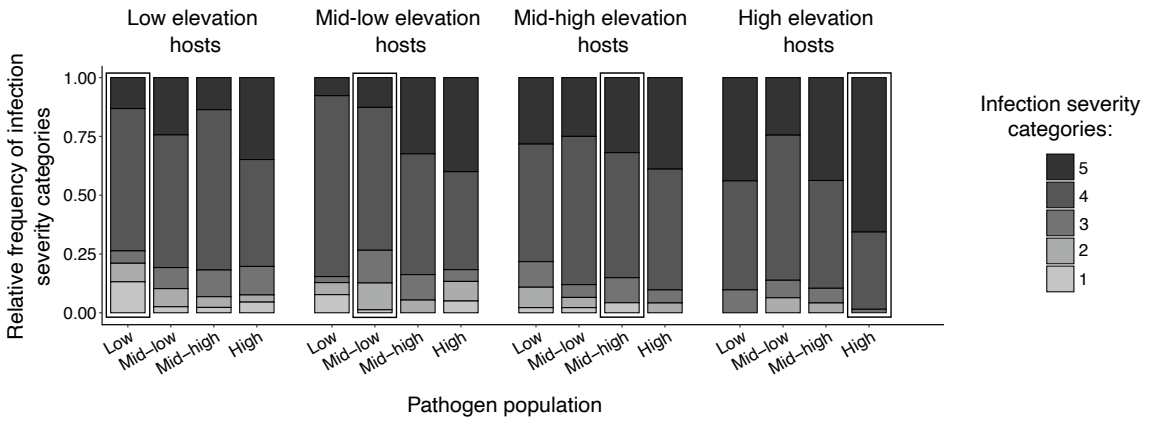

Figure 4: Relative frequency of infection severity categories. Each stacked bar plot shows the relative frequencies of each infection severity category recorded over both experimental blocks for all combinations of host and pathogen populations. Sympatric combinations are indicated by a bracket surrounding the stacked bar plots.

398

Table 1: Analysis of deviance table of the results of the logistic mixed model of the infection outcome of each pair of mildew isolate and plant individual.

Source	χ^2	**D. f.**	**Pr(>χ^2)**
Host population	0.178	3	0.981
Pathogen population	3.016	3	0.389
Host population:Pathogen population	9.077	9	0.430

399

400

Table 2: Analysis of deviance table of the results of the cumulative link mixed model on the disease severity of successful infections of each pair of mildew isolate and plant individual. Significant predictors ($p < 0.05$) are indicated in bold.

Source	**LR χ^2**	**D. f.**	**Pr(>χ^2)**
Block	0.172	1	0.679
Host population	9.574	3	**0.023**
Pathogen population	10.932	3	**0.012**
Block:Host population	9.009	3	**0.029**
Block:Pathogen population	4.432	3	0.218
Host population:Pathogen population	18.910	9	**0.027**
Block:Host population:Pathogen population	10.812	9	0.289

Discussion

Although variation in the intensity of biotic interactions along environmental gradients has frequently been observed (Hargreaves et al., 2019; Paquette & Hargreaves, 2021; Roslin et al., 2017; Zvereva & Kozlov, 2022), whether this leads to differences in reciprocal selection dynamics has been rarely addressed. Here, we experimentally tested whether the direction and strength of local adaptation varied between four populations of the host plant *P. lanceolata* and its fungal pathogen *P. plantaginis* along an altitudinal gradient. The system is characterized by variation in infection prevalence in the natural populations along the elevation gradient. In our field survey, we rarely observed infected host plants at the highest elevation population. In our inoculation study, infection severity was highest and mildew sporulated earliest on plants from the high-elevation population regardless of pathogen origin. This pattern might reflect relaxed natural selection for quantitative disease resistance in high-elevation hosts. Our local adaptation assay revealed that the lowest and highest altitude populations showed opposing signs of local adaptation in infection severity (Fig.4). The high-elevation pathogen population was locally adapted, whereas the low-elevation pathogen population was locally maladapted. Interestingly, the patterns of resistance and virulence mirror the past infection pressure in these populations. Together, these results could also suggest that our study populations are at different stages in a coevolutionary process, which is not unexpected given the cyclical nature of coevolution (Thompson, 2005). This may have implications for shifts of pathogen distributions under climate and land use change.

The *P. lanceolata* populations showed fluctuations in density between seasons, however these differences, while statistically significant, were small. While maximum density showed a clear decrease with increasing elevation (Fig. 1B), the average density was similar. Hence, the

surveyed host populations appear to be stable. In our experiment, we found that all studied populations contained plants that were resistant to some of the tested powdery mildew isolates, while being susceptible to others, suggesting high specificity of the interactions. We did not detect significant differences in qualitative resistance among the host populations. Such a pattern could indicate that either selection for qualitative resistance is similar between our study populations or that gene flow among the populations maintains the observed frequency of resistant plant genotypes. In population genetic models of gene-for-gene dynamics (the genetic basis of qualitative resistance), a cost of resistance is often required for stable coexistence of resistant and susceptible alleles in host populations (Antonovics & Thrall, 1997; but see Thrall & Burdon, 2003). In *P. lanceolata*, Susi & Laine (2015) found that resistance to *P. plantaginis* imposes a cost in the absence of powdery mildew by reducing the size of plants. Such a trade-off could explain why we found both resistant and susceptible plants in every population. Further, in their study, the cost for qualitative resistance was lower than for quantitative resistance. In contrast to qualitative resistance, we found that with increasing elevation of origin, host populations had lower quantitative resistance. Quantitative resistance is typically polygenic and limits pathogen growth rather than preventing infection (Young, 1996). The combined effect of decreasing exposure to powdery mildew infection and the cost of resistance could potentially select against quantitatively resistant individuals. Shorter sporulation times and a higher proportion of chasmothecia on high-elevation hosts further underline the decrease in quantitative resistance traits with elevation. However, we acknowledge that our experimental plants were grown from field collected seeds which carry environment specific maternal effects. Because the experimental patterns of quantitative resistance mirror the infection prevalence observed in the field surveys, we cannot rule out maternal effects as contributors to the observed resistance phenotype. Previous research in this host-pathogen system has indeed documented such effects (Höckerstedt et al., 2020). Importantly, because host–pathogen

interactions in natural populations occur on realized phenotypes rather than genotypes alone, such maternal effects may themselves contribute to ecologically relevant variation in resistance upon which selection acts (Bonduriansky & Day, 2009; Uller, 2008).

Observations of powdery mildew-infected plants were rare on plants above 1600 meters of elevation in our field survey. Similar effects of altitude on disease prevalence were also found in coffee leaf rust (Belachew et al., 2020). Lower temperatures at higher elevations are likely the main cause of the decrease in disease prevalence as they are unfavourable for powdery mildew development (Schnathorst, 1965). We further observed differences between seasons, which may be related to yearly variation in abiotic conditions as well. For example, the low infection pressure in 2019 may have been a result of a drought event in the region in 2018 (Laine, *pers. obs.*). Together, these observations indicate that disease prevalence in the field is driven by environmental constraints. In contrast, our inoculation experiment showed that high-elevation isolates cause the most severe infections. Several mutually non-exclusive mechanisms could explain this pattern (though noting that the experiment was conducted at a temperature more representative of lower elevations; Halliday et al., 2023). First, higher infection severity categories on the Bevan's scale (Bevan et al., 1993) translate to a higher number of fungal spores, which could reflect an adaptation to a shorter growing season and lower host densities at higher altitudes. Second, high-elevation isolates could carry fewer virulence factors and thus bear a lower cost of virulence. Such trade-offs between virulence and growth have been observed in multiple plant pathogens (Bahri et al., 2009; Huang et al., 2006; Montarry et al., 2010). Jointly, the results of the field observations and inoculation study suggest that infection prevalence in the natural population at high elevations is mostly constrained by the environmental context rather than by host or pathogen traits. However, this hypothesis remains to be tested experimentally. Finally, we do not know the relative

distribution of both powdery mildew species in our populations, which has important implications regarding the evolution of resistance in the host. Because *P. plantaginis* and *G. sordidus* belong to different tribes within the powdery mildews (*Erysiphales*) (Kusch et al., 2024; Takamatsu, 2013), we would expect host resistance to be pathogen species specific (Dangl & Jones, 2001) with resistance against each pathogen therefore evolving independently. Future studies, that characterize the pathogen communities and quantify their abundances along elevation gradients will be essential to disentangle the ecological and evolutionary processes that shape disease dynamics in this system.

Our analysis of infection severity of successful infections revealed that high-elevation pathogen isolates were locally adapted, and low-elevation pathogen isolates were locally maladapted. These results suggests that reciprocal selection between hosts and pathogens changes asymmetrically with altitude. Two mutually non-exclusive processes could produce such a pattern. First, genetic drift and gene flow are expected to impact coevolutionary dynamics between hosts and pathogens (Gandon et al., 1997; Gandon & Michalakis, 2002; White et al., 2021). The relative rate of gene flow between hosts and pathogens has been found to predict whether hosts or pathogens are locally adapted (Hoeksema & Forde, 2008). Low-elevation hosts and pathogens are more closely connected to the central distribution of their species. Thus, at a lower elevation, local selection dynamics may be affected to a greater extent by incoming gene flow compared to higher-elevation populations (Höckerstedt et al., 2018) which could swamp local adaptation. Another hypothesis that would predict such a pattern of asymmetry in local adaptation is the coevolutionary selection mosaic (Thompson, 2005). A selection mosaic represents spatial variation in the frequency-dependent interspecific fitness functions among interacting species (Gomulkiewicz et al., 2007; Thompson, 2005). According to the selection mosaic, both the strength and direction of selection vary spatially. Selection

mosaics have been described in ecological interactions such as those between seed predators and pine trees, pollinators and plants, and herbivores and plants (Benkman, 1999; Muola et al., 2010; Soteras et al., 2020). Future work combining cross-infection experiments with genomic analysis, including multiple populations, will reveal the role of gene flow, genetic drift and selection mosaics on eco-evolutionary dynamics between hosts and pathogens (Amandine et al., 2022).

The observed increase of pathogen virulence together with the decrease in quantitative host resistance along elevation raises fundamental questions about trade-offs between investment into growth, reproduction, and virulence/resistance in host pathogen systems across heterogeneous environments (Stearns, 1989). The changing abiotic conditions with elevation may modulate costs and benefits of different life-history strategies, which could drive the evolution of high and low elevation ecotypes in both hosts and pathogens (Turesson, 1922). This idea is particularly relevant in in plant-pathogen systems, where host plants often evolve ecotypes adapted to local conditions (Hufford & Mazer, 2003; Leimu & Fischer, 2008; Savolainen et al., 2007). Pathogens that specialise on specific host ecotypes may simultaneously generate divergence between pathogen populations (Laine et al., 2014). Experimental approaches that manipulate abiotic conditions could test whether divergence in quantitative resistance and virulence confers fitness advantages in low- and high-elevation environments.

The incorporation of the relevant natural context into studies of local adaptation in host-pathogen systems is a powerful approach to further our understanding of the coevolutionary process (Wolinska & King, 2009). Here, we performed an experimental test of local adaptation with populations of a host plant and one of its fungal pathogens along a natural altitudinal

gradient. We showed that varying patterns of local adaptation emerge in heterogeneous environmental conditions over smaller spatial scales. This suggests that varying interaction intensities along elevation may alter selection between interacting species, as predicted by theory (Benkman, 2013; Hochberg & Baalen, 1998). As our study focused on a single elevation gradient, more replicated elevation gradients across regions and species interactions will now be important to determine how general such patterns are. More broadly, the growing body of ecological work suggests that the intensity and outcome of species interactions can shift predictably along environmental gradients (Hargreaves et al., 2020; Roslin et al., 2017; Zvereva & Kozlov, 2022), raising the exciting possibility that elevation and other forms of environmental gradients may generate spatially predictable variation in trajectories of coevolution across a wide range of interacting species.

Author contributions

A-LL, AW and MR conceived and designed the study, FWH collected field observational data with contributions of MR, MR collected field material and carried out the experiment, MG & MR performed PCR genotyping, MR analyzed the data, MR & A-LL drafted the initial version of the manuscript, all authors contributed to the final version of the manuscript.

Acknowledgments

We thank the community of Chur for access to field populations, J. Gehler for support during sample collection, V. Loaiza, K. Raveala, M. Jalo, M. Tiusanen, I. Kohonen, S. Keller, B. Oberholzer, S. Czyżweski and J. Gehler for assistance during field surveys, K. Shimizu and M. Brasser for providing and setting up experimental chambers, J. Wiethase for advice on the

546 statistical analysis of the field survey data, and the members of the Laine lab and Wagner lab
547 for helpful discussions.

548 Funding

549 This work was supported by the University of Zurich and a PhD grant from the University
550 Research Priority Program 'Evolution in Action' to A-LL and AW. A-LL acknowledges
551 funding from the European Research Council (Advanced Grant Co-EvoChange 101097545)
552 and Academy of Finland (362242).

553 Conflict of interest statement

554 The authors have no competing interests to declare.

555 Data and code availability

556 All data and code will be made publicly available upon publication.

557 References

558 Abbate, J. L., & Antonovics, J. (2014). Elevational disease distribution in a natural plant–
559 pathogen system: Insights from changes across host populations and climate. *Oikos*,
560 *123*(9), 1126–1136. https://doi.org/10.1111/oik.01001
561 Alexander, J. M., van Kleunen, M., Ghezzi, R., & Edwards, P. J. (2012). Different genetic
562 clines in response to temperature across the native and introduced ranges of a global
563 plant invader. *Journal of Ecology*, *100*(3), 771–781. https://doi.org/10.1111/j.1365-
564 2745.2011.01951.x

565 Amandine, C., Ebert, D., Stukenbrock, E., Vega, R. C. R. de la, Tiffin, P., Croll, D., & Tellier,
566 A. (2022). Unraveling coevolutionary dynamics using ecological genomics. *Trends in*
567 *Genetics*, *38*(10), 1003–1012. https://doi.org/10.1016/j.tig.2022.05.008
568 Antonovics, J., & Thrall, P. H. (1997). The cost of resistance and the maintenance of genetic
569 polymorphism in host—Pathogen systems. *Proceedings of the Royal Society of London.*
570 *Series B: Biological Sciences*, *257*(1349), 105–110.
571 https://doi.org/10.1098/rspb.1994.0101
572 Arnold, S. J., & Wade, M. J. (1984). On the Measurement of Natural and Sexual Selection:
573 Theory. *Evolution*, *38*(4), 709–719. https://doi.org/10.2307/2408383
574 Ashby, B., Iritani, R., Best, A., White, A., & Boots, M. (2019). Understanding the role of eco-
575 evolutionary feedbacks in host-parasite coevolution. *Journal of Theoretical Biology*,
576 *464*, 115–125. https://doi.org/10.1016/j.jtbi.2018.12.031
577 Bahri, B., Kaltz, O., Leconte, M., de Vallavieille-Pope, C., & Enjalbert, J. (2009). Tracking
578 costs of virulence in natural populations of the wheat pathogen, Puccinia striiformis
579 f.sp.tritici. *BMC Evolutionary Biology*, *9*(1), 26. https://doi.org/10.1186/1471-2148-9-
580 26
581 Bates, D., Mächler, M., Bolker, B., & Walker, S. (2015). Fitting Linear Mixed-Effects Models
582 Using lme4. *Journal of Statistical Software*, *67*, 1–48.
583 https://doi.org/10.18637/jss.v067.i01
584 Belachew, K., Senbeta, G. A., Garedew, W., Barreto, R. W., & Del Ponte, E. M. (2020).
585 Altitude is the main driver of coffee leaf rust epidemics: A large-scale survey in
586 Ethiopia. *Tropical Plant Pathology*, *45*(5), 511–521. https://doi.org/10.1007/s40858-
587 020-00383-4

588 Benkman, C. W. (1999). The Selection Mosaic and Diversifying Coevolution between
589 Crossbills and Lodgepole Pine. *The American Naturalist*, *153*(S5), S75–S91.
590 https://doi.org/10.1086/303213
591 Benkman, C. W. (2013). Biotic interaction strength and the intensity of selection. *Ecology*
592 *Letters*. https://doi.org/10.1111/ele.12138
593 Bevan, J. R., Crute, I. R., & Clarke, D. D. (1993). Variation for virulence in Erysiphe fischeri
594 from Senecio vulgaris. *Plant Pathology*, *42*(4), 622–635.
595 https://doi.org/10.1111/j.1365-3059.1993.tb01543.x
596 Blanquart, F., Kaltz, O., Nuismer, S. L., & Gandon, S. (2013). A practical guide to measuring
597 local adaptation. *Ecology Letters*, *16*(9), 1195–1205. https://doi.org/10.1111/ele.12150
598 Bonduriansky, R., & Day, T. (2009). Nongenetic Inheritance and Its Evolutionary Implications.
599 *Annual Review of Ecology, Evolution, and Systematics*, *40*(Volume 40, 2009), 103–
600 125. https://doi.org/10.1146/annurev.ecolsys.39.110707.173441
601 Brooks, M. E., Kristensen, K., Benthem, K. J. van, Magnusson, A., Berg, C. W., Nielsen, A.,
602 Skaug, H. J., Mächler, M., & Bolker, B. M. (2017). glmmTMB Balances Speed and
603 Flexibility Among Packages for Zero-inflated Generalized Linear Mixed Modeling.
604 *The R Journal*, *9*(2), 378–400.
605 Chaloner, T. M., Gurr, S. J., & Bebber, D. P. (2020). Geometry and evolution of the ecological
606 niche in plant-associated microbes. *Nature Communications*, *11*(1), 2955.
607 https://doi.org/10.1038/s41467-020-16778-5
608 Christensen, R. H. B. (2023). *ordinal: Regression Models for Ordinal Data* (Version 2023.12-
609 4) [Computer software]. https://cran.r-project.org/web/packages/ordinal/index.html
610 *CRAN: Package emmeans*. (n.d.). Retrieved June 13, 2024, from https://cran.r-
611 project.org/web/packages/emmeans/index.html

612 D. C. Lopez-Pascua, L., & Buckling, A. (2008). Increasing productivity accelerates host–
613 parasite coevolution. *Journal of Evolutionary Biology*, *21*(3), 853–860.
614 https://doi.org/10.1111/j.1420-9101.2008.01501.x
615 Dangl, J. L., & Jones, J. D. G. (2001). Plant pathogens and integrated defence responses to
616 infection. *Nature*, *411*(6839), 826–833. https://doi.org/10.1038/35081161
617 Darwin, C. R. (1859). *On the origin of species by means of natural selection, or the*
618 *preservation of favoured races in the struggle for life.* London: John Murray.
619 Duncan, A. B., Dusi, E., Jacob, F., Ramsayer, J., Hochberg, M. E., & Kaltz, O. (2017). Hot
620 spots become cold spots: Coevolution in variable temperature environments. *Journal*
621 *of Evolutionary Biology*, *30*(1), 55–65. https://doi.org/10.1111/jeb.12985
622 Gandon, S., Capowiez, Y., Dubois, Y., Michalakis, Y., & Olivieri, I. (1997). Local adaptation
623 and gene-for-gene coevolution in a metapopulation model. *Proceedings of the Royal*
624 *Society of London. Series B: Biological Sciences*, *263*(1373), 1003–1009.
625 https://doi.org/10.1098/rspb.1996.0148
626 Gandon, S., & Michalakis, Y. (2002). Local adaptation, evolutionary potential and host–
627 parasite coevolution: Interactions between migration, mutation, population size and
628 generation time. *Journal of Evolutionary Biology*, *15*(3), 451–462.
629 https://doi.org/10.1046/j.1420-9101.2002.00402.x
630 George McNew. (1960). The nature, origin, and evolution of parasitism. In *Plant Pathology:*
631 *An Advanced Treatise* (p. 56). Academic Press.
632 Gomulkiewicz, R., Drown, D. M., Dybdahl, M. F., Godsoe, W., Nuismer, S. L., Pepin, K. M.,
633 Ridenhour, B. J., Smith, C. I., & Yoder, J. B. (2007). Dos and don'ts of testing the
634 geographic mosaic theory of coevolution. *Heredity 2007 98:5*, *98*(5), 249–258.
635 https://doi.org/10.1038/sj.hdy.6800949

636 Gomulkiewicz, R., Thompson, J. N., Holt, R. D., Nuismer, S. L., & Hochberg, M. E. (2000).
637 Hot Spots, Cold Spots, and the Geographic Mosaic Theory of Coevolution. *The*
638 *American Naturalist*, *156*(2), 156–174. https://doi.org/10.1086/303382
639 Greischar, M. A., & Koskella, B. (2007). A synthesis of experimental work on parasite local
640 adaptation. *Ecology Letters*, *10*(5), 418–434. https://doi.org/10.1111/j.1461-
641 0248.2007.01028.x
642 Halliday, F. W., Jalo, M., & Laine, A. L. (2021). The effect of host community functional traits
643 on plant disease risk varies along an elevational gradient. *eLife*, *10*.
644 https://doi.org/10.7554/ELIFE.67340
645 Hargreaves, A. L., Germain, R. M., Bontrager, M., Persi, J., & Angert, A. L. (2020). Local
646 Adaptation to Biotic Interactions: A Meta-analysis across Latitudes. *The American*
647 *Naturalist*, *195*(3), 395–411. https://doi.org/10.1086/707323
648 Hargreaves, A. L., Suárez, E., Mehltreter, K., Myers-Smith, I., Vanderplank, S. E., Slinn, H.
649 L., Vargas-Rodriguez, Y. L., Haeussler, S., David, S., Muñoz, J., Almazán-Núñez, R.
650 C., Loughnan, D., Benning, J. W., Moeller, D. A., Brodie, J. F., Thomas, H. J. D., &
651 Morales, P. A. (2019). Seed predation increases from the Arctic to the Equator and from
652 high to low elevations. *Science Advances*. https://doi.org/10.1126/sciadv.aau4403
653 Harrison, E., Laine, A.-L., Hietala, M., & Brockhurst, M. A. (2013). Rapidly fluctuating
654 environments constrain coevolutionary arms races by impeding selective sweeps.
655 *Proceedings of the Royal Society B: Biological Sciences*, *280*(1764), 20130937.
656 https://doi.org/10.1098/rspb.2013.0937
657 Hartig, F. (2025). *DHARMa: Residual Diagnostics for Hierarchical (Multi-Level / Mixed)*
658 *Regression Models* (Version 0.4.7) [Computer software].
659 https://github.com/florianhartig/dharma

660 HERVE, M. (2023). *RVAideMemoire: Testing and Plotting Procedures for Biostatistics*
661 (Version 0.9-83-7) [Computer software]. https://cran.r-
662 project.org/web/packages/RVAideMemoire/index.html
663 Ho, H.-C., Brodersen, J., Gossner, M. M., Graham, C. H., Kaeser, S., Reji Chacko, M.,
664 Seehausen, O., Zimmermann, N. E., Pellissier, L., & Altermatt, F. (2022). Blue and
665 green food webs respond differently to elevation and land use. *Nature Communications*,
666 *13*(1), Article 1. https://doi.org/10.1038/s41467-022-34132-9
667 Hochberg, M. E., & Baalen, M. van. (1998). Antagonistic Coevolution over Productivity
668 Gradients. *The American Naturalist*, *152*(4), 620–634. https://doi.org/10.1086/286194
669 Höckerstedt, L. M., Siren, J. P., & Laine, A. L. (2018). Effect of spatial connectivity on host
670 resistance in a highly fragmented natural pathosystem. *Journal of Evolutionary*
671 *Biology*. https://doi.org/10.1111/jeb.13268
672 Höckerstedt, L., Susi, H., & Laine, A. L. (2020). Effect of maternal infection on progeny
673 growth and resistance mediated by maternal genotype and nutrient availability. *Journal*
674 *of Ecology*. https://doi.org/10.1111/1365-2745.13568
675 Hoeksema, J. D., & Forde, S. E. (2008). A Meta-Analysis of Factors Affecting Local
676 Adaptation between Interacting Species. *The American Naturalist*, *171*(3), 275–290.
677 https://doi.org/10.1086/527496
678 Huang, Y.-J., Li, Z.-Q., Evans, N., Rouxel, T., Fitt, B. D. L., & Balesdent, M.-H. (2006).
679 Fitness Cost Associated with Loss of the AvrLm4 Avirulence Function in
680 Leptosphaeria maculans (Phoma Stem Canker of Oilseed Rape). *European Journal of*
681 *Plant Pathology*, *114*(1), 77–89. https://doi.org/10.1007/s10658-005-2643-4
682 Hufford, K. M., & Mazer, S. J. (2003). Plant ecotypes: Genetic differentiation in the age of
683 ecological restoration. *Trends in Ecology & Evolution*, *18*(3), 147–155.
684 https://doi.org/10.1016/S0169-5347(03)00002-8

685 Jones, J. D. G., & Dangl, J. L. (2006). The plant immune system. *Nature*.
686 https://doi.org/10.1038/nature05286
687 Kawecki, T. J., & Ebert, D. (2004). Conceptual issues in local adaptation. *Ecology Letters*.
688 https://doi.org/10.1111/j.1461-0248.2004.00684.x
689 King, K. C., Delph, L. F., Jokela, J., & Lively, C. M. (2009). The Geographic Mosaic of Sex
690 and the Red Queen. *Current Biology*, *19*(17), 1438–1441.
691 https://doi.org/10.1016/j.cub.2009.06.062
692 Körner, C. (2003). *Alpine Plant Life*. Springer. https://doi.org/10.1007/978-3-642-18970-8
693 Kusch, S., Qian, J., Loos, A., Kümmel, F., Spanu, P. D., & Panstruga, R. (2024). Long-term
694 and rapid evolution in powdery mildew fungi. *Molecular Ecology*, *33*(10), e16909.
695 https://doi.org/10.1111/mec.16909
696 Laine, A.-L. (2005). Spatial scale of local adaptation in a plant-pathogen metapopulation.
697 *Journal of Evolutionary Biology*. https://doi.org/10.1111/j.1420-9101.2005.00933.x
698 Laine, A.-L., Burdon, J. J., Nemri, A., & Thrall, P. H. (2014). *Host ecotype generates*
699 *evolutionary and epidemiological divergence across a pathogen metapopulation*.
700 https://dx.doi.org/10.1098/rspb.2014.0522
701 Lauber, K., Wagner, G., & Gygax, A. (2018). In *Flora Helvetica – Illustrierte Flora der*
702 *Schweiz* (7th ed., p. 1686). Haupt.
703 Leimu, R., & Fischer, M. (2008). A Meta-Analysis of Local Adaptation in Plants. *PLoS ONE*,
704 *3*(12), e4010. https://doi.org/10.1371/journal.pone.0004010
705 Lopez-Pascua, L. D. C., Brockhurst, M. A., & Buckling, A. (2010). Antagonistic coevolution
706 across productivity gradients: An experimental test of the effects of dispersal. *Journal*
707 *of Evolutionary Biology*, *23*(1), 207–211. https://doi.org/10.1111/j.1420-
708 9101.2009.01877.x

709 Louthan, A. M., Doak, D. F., & Angert, A. L. (2015). Where and When do Species Interactions
710 Set Range Limits? *Trends in Ecology & Evolution*, *30*(12), 780–792.
711 https://doi.org/10.1016/j.tree.2015.09.011
712 McDonald, B. A., & Linde, C. (2002). PATHOGEN POPULATION GENETICS,
713 EVOLUTIONARY POTENTIAL, AND DURABLE RESISTANCE. *Annual Review*
714 *of Phytopathology*, *40*(Volume 40, 2002), 349–379.
715 https://doi.org/10.1146/annurev.phyto.40.120501.101443
716 McNew, S. M., Barrow, L. N., Williamson, J. L., Galen, S. C., Skeen, H. R., DuBay, S. G.,
717 Gaffney, A. M., Johnson, A. B., Bautista, E., Ordoñez, P., Schmitt, C. J., Smiley, A.,
718 Valqui, T., Bates, J. M., Hackett, S. J., & Witt, C. C. (2021). Contrasting drivers of
719 diversity in hosts and parasites across the tropical Andes. *Proceedings of the National*
720 *Academy of Sciences*, *118*(12), e2010714118.
721 https://doi.org/10.1073/pnas.2010714118
722 Montarry, J., Hamelin, F. M., Glais, I., Corbière, R., & Andrivon, D. (2010). Fitness costs
723 associated with unnecessary virulence factors and life history traits: Evolutionary
724 insights from the potato late blight pathogen Phytophthora infestans. *BMC*
725 *Evolutionary Biology*, *10*(1), 283. https://doi.org/10.1186/1471-2148-10-283
726 Muola, A., Mutikainen, P., Lilley, M., Laukkanen, L., Salminen, J.-P., & Leimu, R. (2010).
727 Associations of plant fitness, leaf chemistry, and damage suggest selection mosaic in
728 plant–herbivore interactions. *Ecology*, *91*(9), 2650–2659. https://doi.org/10.1890/09-
729 0589.1
730 Nicot, P. C., Bardin, M., & Dik, A. J. (2002). Basic methods for epidemiological studies of
731 powdery mildews: Culture and preservation of isolates, production and delivery of
732 inoculum, and disease assessment. In *The Powdery Mildews: A Comprehensive*

Treatise (Bélanger R. R., Bushnell R. B., Dik A. J. & Carver T. J. W., eds (pp. 83–99). The American Phytopathological Society.

Paquette, A., & Hargreaves, A. L. (2021). Biotic interactions are more often important at species' warm versus cool range edges. *Ecology Letters*, *24*(11), 2427–2438. https://doi.org/10.1111/ele.13864

Penczykowski, R. M., & Sieg, R. D. (2021). Plantago spp. As Models for Studying the Ecology and Evolution of Species Interactions across Environmental Gradients. *The American Naturalist*, *198*(1), 158–176. https://doi.org/10.1086/714589

Poland, J. A., Balint-Kurti, P. J., Wisser, R. J., Pratt, R. C., & Nelson, R. J. (2009). Shades of gray: The world of quantitative disease resistance. *Trends in Plant Science*, *14*(1), 21–29. https://doi.org/10.1016/j.tplants.2008.10.006

Pulgarín-R, P. C., Gómez, J. P., Robinson, S., Ricklefs, R. E., & Cadena, C. D. (2018). Host species, and not environment, predicts variation in blood parasite prevalence, distribution, and diversity along a humidity gradient in northern South America. *Ecology and Evolution*, *8*(8), 3800–3814. https://doi.org/10.1002/ece3.3785

R: The R Project for Statistical Computing. (n.d.). Retrieved May 17, 2023, from https://www.r-project.org/

Roslin, T., Hardwick, B., Novotny, V., Petry, W. K., Andrew, N. R., Asmus, A., Barrio, I. C., Basset, Y., Boesing, A. L., Bonebrake, T. C., Cameron, E. K., Dáttilo, W., Donoso, D. A., Drozd, P., Gray, C. L., Hik, D. S., Hill, S. J., Hopkins, T., Huang, S., … Slade, E. M. (2017). Latitudinal gradients: Higher predation risk for insect prey at low latitudes and elevations. *Science*. https://doi.org/10.1126/science.aaj1631

Savolainen, O., Pyhäjärvi, T., & Knürr, T. (2007). Gene Flow and Local Adaptation in Trees. *Annual Review of Ecology, Evolution, and Systematics*, *38*(Volume 38, 2007), 595–619. https://doi.org/10.1146/annurev.ecolsys.38.091206.095646

758 Schnathorst, W. C. (1965). Environmental Relationships in the Powdery Mildews. *Annual*
759 *Review of Phytopathology*, *3*(Volume 3, 1965), 343–366.
760 https://doi.org/10.1146/annurev.py.03.090165.002015
761 Soteras, F., Rubini Pisano, M. A., Bariles, J. B., Moré, M., & Cocucci, A. A. (2020).
762 Phenotypic selection mosaic for flower length influenced by geographically varying
763 hawkmoth pollinator proboscis length and abiotic environment. *New Phytologist*,
764 *225*(2), 985–998. https://doi.org/10.1111/nph.16192
765 Stearns, S. C. (1989). Trade-Offs in Life-History Evolution. *Functional Ecology*, *3*(3), 259–
766 268. https://doi.org/10.2307/2389364
767 Stevens, R. B. (1960). CHAPTER 10—Cultural Practices in Disease Control. In J. G. Horsfall
768 & A. E. Dimond (Eds.), *Plant Pathology* (pp. 357–429). Academic Press.
769 https://doi.org/10.1016/B978-0-12-395678-1.50016-3
770 Susi, H., & Laine, A. L. (2015). The effectiveness and costs of pathogen resistance strategies
771 in a perennial plant. *Journal of Ecology*. https://doi.org/10.1111/1365-2745.12373
772 Tack, A. J. M., & Laine, A. L. (2014). Ecological and evolutionary implications of spatial
773 heterogeneity during the off-season for a wild plant pathogen. *New Phytologist*.
774 https://doi.org/10.1111/nph.12646
775 Takamatsu, S. (2013). Molecular phylogeny reveals phenotypic evolution of powdery mildews
776 (Erysiphales, Ascomycota). *Journal of General Plant Pathology*, *79*(4), 218–226.
777 https://doi.org/10.1007/s10327-013-0447-5
778 Thompson, J. N. (2005). The Geographic Mosaic of Coevolution. In *The Geographic Mosaic*
779 *of Coevolution*. University of Chicago Press. https://doi.org/10.7208/9780226118697
780 Thrall, P. H., & Burdon, J. J. (1997). Host-Pathogen Dynamics in a Metapopulation Context:
781 The Ecological and Evolutionary Consequences of Being Spatial. *Journal of Ecology*,
782 *85*(6), 743–753. https://doi.org/10.2307/2960598

783 Thrall, P. H., & Burdon, J. J. (2003). Evolution of virulence in a plant host-pathogen
784 metapopulation. *Science*. https://doi.org/10.1126/science.1080070
785 Toju, H. (2008). FINE-SCALE LOCAL ADAPTATION OF WEEVIL MOUTHPART
786 LENGTH AND CAMELLIA PERICARP THICKNESS: ALTITUDINAL
787 GRADIENT OF A PUTATIVE ARMS RACE. *Evolution*, *62*(5), 1086–1102.
788 https://doi.org/10.1111/j.1558-5646.2008.00341.x
789 Tollenaere, C., & Laine, A. L. (2013). Investigating the production of sexual resting structures
790 in a plant pathogen reveals unexpected self-fertility and genotype-by-environment
791 effects. *Journal of Evolutionary Biology*. https://doi.org/10.1111/jeb.12169
792 Turesson, G. (1922). The Genotypical Response of the Plant Species to the Habitat. *Hereditas*,
793 *3*(3), 211–350. https://doi.org/10.1111/j.1601-5223.1922.tb02734.x
794 Uller, T. (2008). Developmental plasticity and the evolution of parental effects. *Trends in*
795 *Ecology & Evolution*, *23*(8), 432–438. https://doi.org/10.1016/j.tree.2008.04.005
796 White, P. S., Arslan, D., Kim, D., Penley, M., & Morran, L. (2021). Host genetic drift and
797 adaptation in the evolution and maintenance of parasite resistance. *Journal of*
798 *Evolutionary Biology*, *34*(5), 845–851. https://doi.org/10.1111/jeb.13785
799 Wolinska, J., & King, K. C. (2009). Environment can alter selection in host-parasite
800 interactions. *Trends in Parasitology*. https://doi.org/10.1016/j.pt.2009.02.004
801 Young, N. D. (1996). QTL MAPPING AND QUANTITATIVE DISEASE RESISTANCE IN
802 PLANTS. In *Annual Review of Phytopathology* (Vol. 34, Issue Volume 34, 1996, pp.
803 479–501). Annual Reviews.
804 https://doi.org/https://doi.org/10.1146/annurev.phyto.34.1.479
805 Zvereva, E. L., & Kozlov, M. V. (2021). Latitudinal gradient in the intensity of biotic
806 interactions in terrestrial ecosystems: Sources of variation and differences from the

diversity gradient revealed by meta-analysis. *Ecology Letters*, *24*(11), 2506–2520. https://doi.org/10.1111/ele.13851

Zvereva, E. L., & Kozlov, M. V. (2022). Meta-analysis of elevational changes in the intensity of trophic interactions: Similarities and dissimilarities with latitudinal patterns. *Ecology Letters*, *25*(9), 2076–2087. https://doi.org/10.1111/ele.14090

Supplementary materials

Supplementary Methods

Powdery mildew species identification

To verify the species of the 11 mildew isolates used for the cross-inoculation experiment, conidial spore samples were collected for genomic DNA (gDNA) extraction using a simple and rapid method based on grinding isolated material submerged in lysis buffer, followed by a magnetic bead gDNA purification. In brief: We added 500 µl CD1 lysis buffer (DNeasy PowerSoil Pro Kit, QIAGEN, No. 47014) to a 1.5 ml DNA LoBind tube (Eppendorf No. EP0030108051) containing a single leaf scraping. To grind the isolated material in the lysis buffer we added 300 µl sterile 1 mm diameter garnet particles (Stratech Scientific Ltd, No. 11079110gar-BSP) and three 4 mm sterile metal bearings (Simply Bearings UK, grade 1000 hardened 1010 Carbon steel ball bearings) to the lysis tube. We vortexed the tube briefly and transferred the tube for 2 minutes at a frequency of 25 Hz on the QIAGEN TissueLyzer II. After grinding we centrifuged the tube for 5 minutes at 15,000 rpm in a tabletop centrifuge and transferred the supernatant to a new tube. The gDNA of the supernatant was cleaned using a 1.0 x ratio of MagBio HighPrep beads (MagBio, No. AC60050): we added 400 µl magnetic particles to the supernatant, bound the gDNA for 5 minutes to the beads, washed the beads three times in 1 ml 70 % (v/v) ethanol, removed the ethanol completely, dried the beads for 2

minutes and eluted the gDNA for 5 minutes in 50 µl 1x TE buffer. We quantified the extracted gDNA using Qubit dsDNA Broad Range Kit reagents (ThermoFisher, No.Q32853) and used 1 µl extracted gDNA immediately for PCR.

We amplified and sequenced the ITS 1 region, a universal fungal DNA barcode, using primers ITSF1 (5'-CTTGGTCATTTAGAGGAAGTAA-3') and ITS4 (5'-TCCTCCGCTTATTGATATGC-3'). Amplification of the DNA of each sample was performed in a final reaction volume of 50 µl containing 1 x Kapa HiFi Fidelity Buffer, 0.3 µM ITS1F primer, 0.3 µM ITS4 primer, 0.3 µM dNTPs, 1 Unit Kapa HiFi polymerase, 1 µl DNA extract and DNase/Rnase-free molecular biology grade water. The reactions were subjected to an initial denaturation step of three minutes at 95° C, followed by 30 cycles of 30 seconds of denaturation at 95° C, 30 seconds of primer annealing at 65° C, 30 seconds of elongation at 72° C and ended with a final elongation step for five minutes at 72° C. The amplified products were analysed on a 1% agarose gel stained with GelRed (Biotium, USA) and visualized using the Bio-Rad Gel Doc XR + imaging system (Bio-Rad Laboratories, USA) before shipment to Microsynth AG (Balgach, Switzerland) for Sanger Sequencing. The obtained ITS sequences were controlled for quality using the SnapGene software (www.snapgene.com) through visual inspection of the chromatogram, and a nucleotide BLAST search was conducted against the NCBI nucleotide database (Madden, 2003) to assign a species to a sample. The scientific name of the blast alignment with the highest score was used to assign the sample to either *P. plantaginis* or *G. sordidus*. All 11 isolates were identified as *P. plantaginis*.

References

Madden, T. (2003) The BLAST Sequence Analysis Tool. In *The NCBI Handbook [Internet]*. National Center for Biotechnology Information (US).

Supplementary Figures

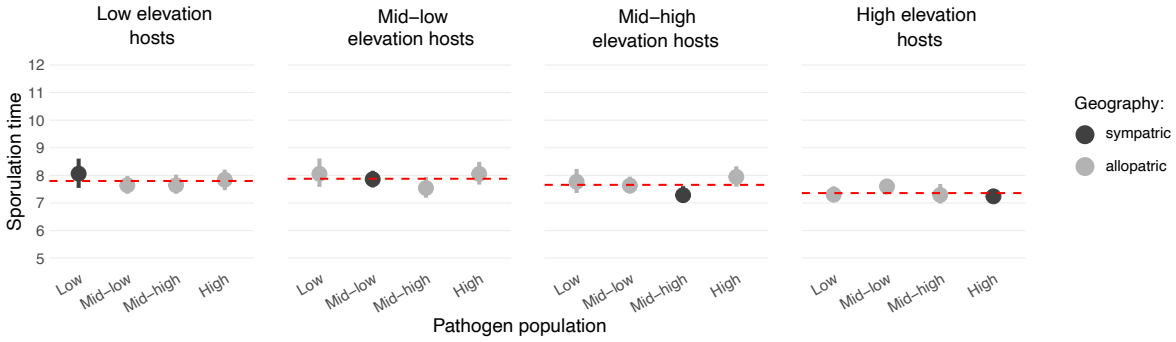

Supplementary Figure 1: Sporulation time of successful infections of sympatric or allopatric host-pathogen pairings. Points show the mean sporulation time between experimental blocks for each comination of host and pathogen population. Error bars indicate the standard error of the mean. The sympatric population combinations are marked in dark grey.

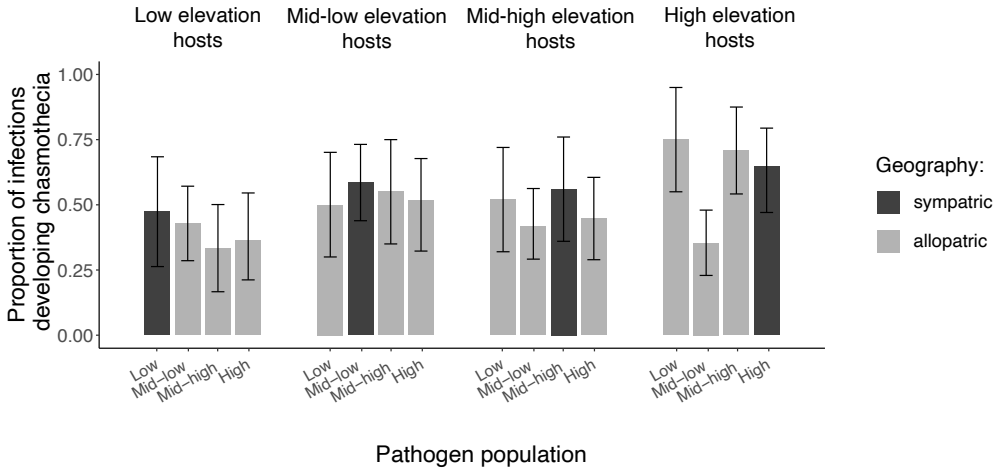

Supplementary Figure 2: Proportion of successful infections developing chasmothecia of sympatric or allopatric host-pathogen pairings. Bar plot shows the proportion of infected hosts with the error bars indicating the standard error of the mean. The sympatric population combinations are marked in dark grey.

Supplementary Tables

Supplementary Table 1: Type II ANOVA χ^2 results of the LMM testing the effect of season and population on host abundance.

Source	χ^2	**Df**	**Pr(>χ^2)**
Population	4.189	3	0.242
Season	11.092	2	0.004
Population:Season	22.691	6	0.001

Supplementary Table 2: Contrasts between season effects on host abundance.

Season contrast	**estimate**	**SE**	**df**	**t.ratio**	**p.value**
Season2019 - Season2020	2.52	1.034	36	2.437	0.051
Season2019 - Season2021	-0.382	1.034	36	-0.37	0.928
Season2020 - Season2021	-2.902	1.034	36	-2.807	0.021

Supplementary Table 3: Contrasts between season effects within each population on host abundance.

Season contrast	**Population**	**estimate**	**SE**	**df**	**t.ratio**	**p.value**
Season2019 - Season2020	Low	-0.841	1.794	36	-0.469	0.886
Season2019 - Season2021	Low	-5.79	1.794	36	-3.228	0.007

Season2020 - Season2021	Low	-4.948	1.794	36	-2.759	0.024
Season2019 - Season2020	Mid-low	6.199	1.938	36	3.199	0.008
Season2019 - Season2021	Mid-low	3.403	1.938	36	1.756	0.199
Season2020 - Season2021	Mid-low	-2.796	1.938	36	-1.443	0.33
Season2019 - Season2020	Mid-high	1.033	2.122	36	0.487	0.878
Season2019 - Season2021	Mid-high	-4.122	2.122	36	-1.942	0.142
Season2020 - Season2021	Mid-high	-5.156	2.122	36	-2.429	0.052
Season2019 - Season2020	High	3.688	2.373	36	1.554	0.278
Season2019 - Season2021	High	4.979	2.373	36	2.098	0.104
Season2020 - Season2021	High	1.292	2.373	36	0.544	0.85

862

Supplementary Table 4: Type II ANOVA χ^2 results of the GLMM testing the effect of season and population on the number of powdery mildew infected plants.

Source	χ^2	Df	Pr(>χ^2)
Population	39.788	3	<0.001
Season	32.812	2	<0.001

863

Supplementary Table 5: Contrasts between population effects and season effects on the number of powdery mildew infected hosts.

Population contrasts	ratio	SE	df	z.ratio	p.value
Low / Mid-low	1.298	0.522	Inf	0.649	0.916
Low / Mid-high	4.321	1.823	Inf	3.47	0.003
Low / High	36.453	23.445	Inf	5.591	<0.001
Mid-low / Mid-high	3.328	1.421	Inf	2.816	0.025
Mid-low / High	28.076	18.253	Inf	5.13	<0.001
Mid-high / High	8.435	5.63	Inf	3.195	0.008
Season contrasts					
Season2019 / Season2020	0.101	0.042	Inf	-5.579	<0.001
Season2019 / Season2021	0.179	0.073	Inf	-4.196	<0.001
Season2020 / Season2021	1.767	0.681	Inf	1.477	0.302

864

Supplementary Table 6: Report table of logistic mixed regression model of infection status

Parameter	Coefficie	CI	CI_low	CI_high	z	p	Effects	Group	Compone
(Intercept)	7.844	0.950	3.823	11.866	3.823	0.000	fixed	0.000	conditiona
Host population [Mid-low]	0.186	0.950	-5.073	5.445	0.069	0.945	fixed	0.000	conditiona
Host population [Mid-high]	2.622	0.950	-2.724	7.967	0.961	0.336	fixed	0.000	conditiona
Host population [High]	0.760	0.950	-4.160	5.679	0.303	0.762	fixed	0.000	conditiona
Pathogen population [Mid-low]	0.868	0.950	-1.051	2.787	0.886	0.375	fixed	0.000	conditiona
Pathogen population [Mid-high]	2.345	0.950	-0.006	4.697	1.955	0.051	fixed	0.000	conditiona
Pathogen population [High]	1.347	0.950	-0.702	3.397	1.289	0.198	fixed	0.000	conditiona
Host population [Mid-low] × Pathogen population [Mid-low]	-0.362	0.950	-3.400	2.676	-0.234	0.815	fixed	0.000	conditiona
Host population [Mid-high] × Pathogen population [Mid-low]	-2.121	0.950	-5.498	1.256	-1.231	0.218	fixed	0.000	conditiona
Host population [High] × Pathogen population [Mid-low]	0.968	0.950	-1.847	3.784	0.674	0.500	fixed	0.000	conditiona
Host population [Mid-low] × Pathogen population [Mid-high]	-3.201	0.950	-6.671	0.269	-1.808	0.071	fixed	0.000	conditiona
Host population [Mid-high] × Pathogen population [Mid-high]	-2.345	0.950	-6.351	1.661	-1.147	0.251	fixed	0.000	conditiona
Host population [High] × Pathogen population [Mid-high]	-0.510	0.950	-3.769	2.749	-0.307	0.759	fixed	0.000	conditiona
Host population [Mid-low] × Pathogen population [High]	-0.658	0.950	-3.906	2.589	-0.397	0.691	fixed	0.000	conditiona
Host population [Mid-high] × Pathogen population [High]	-1.793	0.950	-5.357	1.772	-0.986	0.324	fixed	0.000	conditiona
Host population [High] × Pathogen population [High]	-0.218	0.950	-3.186	2.749	-0.144	0.885	fixed	0.000	conditiona
NA	11.795	0.950	NA	NA	NA	NA	random	Plant.geno	conditiona
NA	0.280	0.950	NA	NA	NA	NA	random	Pathogen.i	conditiona
NA	NA	NA	NA	NA	NA	NA	NA	NA	NA
AIC	NA	NA	NA	NA	NA	NA	NA	NA	NA
AICc	NA	NA	NA	NA	NA	NA	NA	NA	NA
BIC	NA	NA	NA	NA	NA	NA	NA	NA	NA
R2 (conditional)	NA	NA	NA	NA	NA	NA	NA	NA	NA
R2 (marginal)	NA	NA	NA	NA	NA	NA	NA	NA	NA
Sigma	NA	NA	NA	NA	NA	NA	NA	NA	NA
Log_loss	NA	NA	NA	NA	NA	NA	NA	NA	NA

Std_Coeff	Std_Coeff	Std_Coeff	Fit
7.844	3.823	11.866	NA
0.186	-5.073	5.445	NA
2.622	-2.724	7.967	NA
0.760	-4.160	5.679	NA
0.868	-1.051	2.787	NA
2.345	-0.006	4.697	NA
1.347	-0.702	3.397	NA
-0.362	-3.400	2.676	NA
-2.121	-5.498	1.256	NA
0.968	-1.847	3.784	NA
-3.201	-6.671	0.269	NA
-2.345	-6.351	1.661	NA
-0.510	-3.769	2.749	NA
-0.658	-3.906	2.589	NA
-1.793	-5.357	1.772	NA
-0.218	-3.186	2.749	NA
NA	NA	NA	NA
NA	NA	NA	NA
NA	NA	NA	NA
NA	NA	NA	346.361
NA	NA	NA	347.428
NA	NA	NA	427.221
NA	NA	NA	0.977
NA	NA	NA	0.006
NA	NA	NA	1.000
NA	NA	NA	0.130

Supplementary Table 7: Contrasts between host and pathogen population effects on the infection severity category of successful infections over both experimental blocks.

Host population contrast	**OR**	**OR 95% CI**	**p.value**
Low - Mid-low	0.807	[0.346, 1.878]	0.959
Low - Mid-high	0.484	[0.215, 1.089]	0.296
Low - High	0.257	[0.114, 0.576]	0.005
Mid-low - Mid-high	0.600	[0.260, 1.385]	0.628
Mid-low - High	0.318	[0.138, 0.733]	0.036
Mid-high - High	0.531	[0.239, 1.176]	0.401
Pathogen population contrast			
Low - Mid-low	0.976	[0.532, 1.789]	1.000
Low - Mid-high	0.616	[0.306, 1.240]	0.527
Low – High	0.337	[0.177, 0.643]	0.005
Mid-low - Mid-high	0.632	[0.346, 1.154]	0.441
Mid-low – High	0.346	[0.201, 0.593]	0.001
Mid-high - High	0.547	[0.289, 1.037]	0.250

Supplementary Table 8: Contrasts between host and pathogen populations of the ordinal regression model of infection severity. The contrasts are conditional on the host or pathogen population respectively.

Pathogen population contrast	Host.population	OddsRatio	OR 95% CI	p.value
Low - Mid-low	Low	0.468	[0.189, 1.16]	0.356
Low - Mid-high	Low	0.55	[0.198, 1.528]	0.66
Low - High	Low	0.28	[0.109, 0.719]	0.041
Mid-low - Mid-high	Low	1.173	[0.489, 2.814]	0.984
Mid-low - High	Low	0.597	[0.271, 1.314]	0.575
Mid-high - High	Low	0.509	[0.204, 1.269]	0.469
Low - Mid-low	Mid-low	0.981	[0.404, 2.384]	1
Low - Mid-high	Mid-low	0.343	[0.119, 0.983]	0.191
Low - High	Mid-low	0.313	[0.121, 0.813]	0.08
Mid-low - Mid-high	Mid-low	0.349	[0.14, 0.875]	0.111
Mid-low - High	Mid-low	0.319	[0.143, 0.714]	0.028
Mid-high - High	Mid-low	0.913	[0.343, 2.434]	0.998
Low - Mid-low	Mid-high	0.871	[0.367, 2.069]	0.989
Low - Mid-high	Mid-high	0.756	[0.279, 2.05]	0.947
Low - High	Mid-high	0.468	[0.188, 1.16]	0.356

Mid-low - Mid-high	Mid-high	0.867	[0.366, 2.055]	0.988
Mid-low - High	Mid-high	0.536	[0.251, 1.145]	0.373
Mid-high - High	Mid-high	0.619	[0.25, 1.531]	0.727
Low - Mid-low	High	2.263	[0.919, 5.573]	0.285
Low - Mid-high	High	1.012	[0.364, 2.818]	1
Low - High	High	0.316	[0.119, 0.839]	0.095
Mid-low - Mid-high	High	0.447	[0.19, 1.054]	0.255
Mid-low - High	High	0.14	[0.062, 0.313]	0
Mid-high - High	High	0.312	[0.122, 0.798]	0.071
Host population contrast	**Pathogen.population**			
Low - Mid-low	Low	0.734	[0.23, 2.342]	0.954
Low - Mid-high	Low	0.336	[0.109, 1.041]	0.232
Low - High	Low	0.144	[0.045, 0.458]	0.006
Mid-low - Mid-high	Low	0.459	[0.148, 1.424]	0.532
Mid-low - High	Low	0.196	[0.062, 0.626]	0.03
Mid-high - High	Low	0.429	[0.14, 1.314]	0.448
Low - Mid-low	Mid-low	1.536	[0.582, 4.054]	0.822
Low - Mid-high	Mid-low	0.626	[0.244, 1.606]	0.764
Low - High	Mid-low	0.696	[0.275, 1.766]	0.871

Mid-low - Mid-high	Mid-low	0.407	[0.157, 1.056]	0.251
Mid-low - High	Mid-low	0.453	[0.177, 1.162]	0.352
Mid-high - High	Mid-low	1.113	[0.448, 2.765]	0.996
Low - Mid-low	Mid-high	0.457	[0.145, 1.439]	0.539
Low - Mid-high	Mid-high	0.462	[0.156, 1.373]	0.506
Low - High	Mid-high	0.266	[0.09, 0.78]	0.075
Mid-low - Mid-high	Mid-high	1.011	[0.32, 3.19]	1
Mid-low - High	Mid-high	0.58	[0.186, 1.811]	0.785
Mid-high - High	Mid-high	0.574	[0.195, 1.691]	0.745
Low - Mid-low	High	0.821	[0.289, 2.336]	0.983
Low - Mid-high	High	0.563	[0.208, 1.519]	0.668
Low - High	High	0.163	[0.059, 0.453]	0.003
Mid-low - Mid-high	High	0.685	[0.245, 1.918]	0.889
Mid-low - High	High	0.198	[0.069, 0.571]	0.014
Mid-high - High	High	0.29	[0.106, 0.79]	0.073

867

868

Supplementary Table 9: Estimated marginal mean infection severity categories of host and pathogen population pairs.

Pathogen population	**Host population**	**Mean infection severity category**	**SE**	**asymp. LCL**	**asymp. UCL**
Low	Low	3.518	0.219	3.089	3.946

Mid-low	Low	3.87	0.142	3.592	4.149
Mid-high	Low	3.813	0.171	3.478	4.148
High	Low	4.058	0.137	3.79	4.327
Low	Mid-low	3.677	0.204	3.277	4.077
Mid-low	Mid-low	3.702	0.161	3.386	4.018
Mid-high	Mid-low	4.094	0.163	3.774	4.414
High	Mid-low	4.121	0.145	3.836	4.406
Low	Mid-high	3.988	0.16	3.676	4.301
Mid-low	Mid-high	4.042	0.125	3.797	4.287
Mid-high	Mid-high	4.091	0.15	3.797	4.385
High	Mid-high	4.251	0.127	4.002	4.5
Low	High	4.279	0.149	3.988	4.571
Mid-low	High	4.003	0.125	3.757	4.248
Mid-high	High	4.276	0.141	3.999	4.553
High	High	4.617	0.102	4.417	4.817

869

Supplementary Table 10: Contrasts between host populations and experimental block of ordinal regression of infection severity

contrast	**Host.population**	**OR 95% CI**	**OddsRatio**	**p.value**
Block1 - Block2	Low	[0.434, 1.276]	0.744	0.283
Block1 - Block2	Mid-low	[0.268, 0.83]	0.471	0.009
Block1 - Block2	Mid-high	[0.888, 2.532]	1.5	0.129

Block1 - Block2	High	[0.641, 1.916]	1.109	0.712

Supplementary Table 11: Type II ANOVA χ^2 results of linear mixed model of sporulation time.

Source	**Chisq**	**Df**	**Pr(>Chisq)**
Host.population	7.969	3	0.047
Pathogen.population	4.824	3	0.185
Block	0.979	1	0.322
Host.population:Pathogen.population	10.465	9	0.314
Host.population:Block	0.654	3	0.884
Pathogen.population:Block	0.720	3	0.868
Host.population:Pathogen.population:Block	5.833	9	0.756

Supplementary Table 12: Contrasts of host populations of linear regression of sporulation time.

contrast	**estimate**	**SE**	**df**	**lower.CL**	**upper.CL**	**t.ratio**	**p.value**
Low - (Mid-low)	-0.098	0.215	50	-0.670	0.474	-0.455	0.968
Low - (Mid-high)	0.172	0.205	49	-0.373	0.716	0.839	0.836
Low - High	0.489	0.205	51	-0.056	1.035	2.381	0.094

(Mid-low) - (Mid-high)	0.270	0.209	47	-0.287	0.826	1.291	0.573
(Mid-low) - High	0.587	0.210	49	0.030	1.144	2.801	0.035
(Mid-high) - High	0.317	0.199	48	-0.212	0.847	1.597	0.390

873

Supplementary Table 13: Type II ANOVA χ^2 results of logistic mixed model of chasmothecia presence.

Source	**Chisq**	**Df**	**Pr(>Chisq)**
Host population	2.703	3.000	0.440
Pathogen population	4.217	3.000	0.239
Host population:Pathogen population	15.695	9.000	0.074

874